International Journal of Solids and Structures 216 (2021) 136–144

Contents lists available at ScienceDirect

International Journal of Solids and Structures

journal homepage: www.elsevier.com/locate/ijsolstr

Temperature, thermal flux and thermal stress distribution around an elliptic cavity with temperature-dependent material properties

Song Haopeng *, Xie Kunkun, Gao Cunfa

State Key Laboratory of Mechanics and Control of Mechanical Structures, Nanjing University of Aeronautics and Astronautics, Nanjing 210016, China

ARTICLE INFO

Article history:
Received 24 September 2020
Received in revised form 12 December 2020
Accepted 10 January 2021
Available online 22 January 2021

Keywords:
Temperature-dependent
Elliptic cavity
Thermal conductivity
Thermal stress
Stress intensity factors

ABSTRACT

Temperature is an important factor affecting the physical and chemical properties of materials, especially when the temperature changes significantly, such as in the process of heat conduction. The corresponding changes of material properties greatly complicate the distribution of temperature and thermal stress, and make it much more difficult to accurately solve the thermal-elastic field. Using the generalized complex variable method, the thermal-elastic problem of an elliptic cavity embedded in an infinite medium has been analyzed in this paper, with the temperature dependence of thermal conductivity, elastic modulus and thermal expansion coefficient fully accounted for. The temperature, thermal flux and thermoelastic fields have been obtained analytically. The analytical and numerical results show that thermal flux solution is consistent with the temperature independent case, while the temperature and thermal stress solutions are much more complicated. When the elliptical cavity degenerates into a crack, Mode I thermal stress intensity factor K_1 has a tiny negative value, which indicates that thermal flux can actually close the crack slightly. In addition, both K_1 and K_2 vary nonlinearly with remote thermal loads, and depend on $3/2, 5/2$ and $7/2$ power of crack length. These results provide a powerful tool for the failure and reliability analysis of temperature dependent materials.

1. Introduction

As one of the most basic forms of energy, heat widely exists in various systems and devices (Li et al., 2012, 2003). The flow of heat is accompanied by the change of temperature and has a profound impact on its carrier, namely the medium itself. First of all, temperature affects the microstructure and chemical composition of the medium, thus affecting its thermal conductivity, electrical conductivity, elastic modulus, thermal expansion coefficient, hardness, yield strength and rupture strength etc. (Aksamija and Knezevic, 2011; Xie et al., 2014; Liu et al., 2012; Rajabi et al., 2016; Huaijie et al., 2018; Ezzat et al., 2014).

In addition, the thermal expansion of different positions and directions caused by temperature change may not be compatible, thus resulting in significant thermal stress and failure problems (Hasebe and Wang, 2005; Florence and Goodier, 1960; Sih, 1962; Sih, 1965; Wilson and Yu, 1979; Sherief and Ezzat, 1994; Ezzat and Awad, 2010). For examples, Abbas and Marin (2017) consider the problem of a two-dimensional thermoelastic half-space in the context of generalized thermoelastic theory with one relaxation time. Dag established two new computational method based on the J(k)-integral (Dag, 2007; Dag et al., 2010) and J(1)-integral (Dag et al. (2013)) to calculate crack tip parameters for functionally graded materials (FGMs) that are subjected to mixed-mode thermal loading. Alonso et al., 1999 characterized a nontrivial features of heat conduction. While the heat conductivity is well defined in the thermodynamic limit, a linear gradient appears only for quite small temperature differences, and a thermal stress fracture mode of material removal by laser cutting is researched by Molian et al. (2008). Also, in our previous work, the electric, heat conduction and corresponding progressive thermal stress distribution have been discussed (Xie et al., 2019; Song et al., 2020). However, in order to simplify the calculation, the temperature independent material properties has been used in these studies.

In the experiment, the thermal conductivity, elastic modulus and thermal expansion coefficient of most materials change significantly with temperature, which greatly complicates the analysis and calculation of heat conduction and thermal stress. Some numerical simulation methods have been developed to study thermoelasticity (Abbas and Youssef, 2012; Abbas, 2014), thermal stress (Abbas, 2014) and material properties (Ezzat et al., 2004) in temperature dependent cases. However, the numerical results can not give the formula relationship between the parameters

* Corresponding author.
E-mail address: hpsong@nuaa.edu.cn (S. Haopeng).

https://doi.org/10.1016/j.ijsolstr.2021.01.010
0020-7683/

and the final field distributions. It is thus highly desirable if a general analytic method for temperature and thermoelastic fields in materials with temperature-dependent properties can be derived.

Obviously, the temperature dependence of material properties can significantly complicate the governing equations, including heat conduction equations, equilibrium differential equations and compatibility equations, and make it very difficult to solve these equations analytically. According to our best knowledge, although the temperature dependence of material properties is very important in large temperature gradient problems, the analytical research on such problems is still very rare.

In the current study, the thermal-elastic problem of an elliptic cavity embedded in an infinite medium has been analyzed, with the temperature dependence of thermal conductivity, elastic modulus and thermal expansion coefficient fully accounted for. The temperature, thermal flux and thermoelastic fields have been obtained analytically. The analytical and numerical results show that thermal flux solution is consistent with the temperature independent case, while the temperature and thermal stress solutions are much more complicated. In addition, both K_1 and K_2 vary nonlinearly with remote thermal load, and depend on $a^{3/2}, a^{5/2}$ and $a^{7/2}$ power of crack length.

2. Governing equations and general treatment

2.1. Heat conduction equation

In a two-dimensional plane, when the thermal conductivity of the medium changes with temperature, the heat conduction equations are

$$\begin{aligned} J_{Qx} &= -\kappa(T)\frac{\partial T}{\partial x}, \\ J_{Qy} &= -\kappa(T)\frac{\partial T}{\partial y}, \end{aligned} \tag{1}$$

where T is temperature field, and $\kappa(T)$ represents thermal conductivity, which varies with T arbitrarily.

In the following analysis, we consider that heat energy is conserved in this system, such that thermal flux are divergence-free:

$$\nabla \cdot J_Q = 0. \tag{2}$$

2.2. Compatibility equation and equilibrium differential equation

The thermal expansion of different positions and directions caused by temperature change may not be compatible, thus resulting in significant thermal stress. For solving this thermal stress, we first list the compatible equations of thermoelasticity

$$\frac{\partial^2 \gamma_{xy}}{\partial x \partial y} = \frac{\partial^2 \varepsilon_x}{\partial y^2} + \frac{\partial^2 \varepsilon_y}{\partial x^2}, \tag{3}$$

and the geometric equations are

$$\begin{aligned} \varepsilon_x &= \frac{\partial u}{\partial x}, \\ \varepsilon_y &= \frac{\partial v}{\partial y}, \\ \gamma_{xy} &= \frac{\partial v}{\partial x} + \frac{\partial u}{\partial y}, \end{aligned} \tag{4}$$

The rest equations to be satisfied are the equilibrium differential equations, which are also listed here

$$\begin{aligned} \frac{\partial \sigma_x}{\partial x} + \frac{\partial \sigma_{xy}}{\partial y} &= 0, \\ \frac{\partial \sigma_y}{\partial y} + \frac{\partial \sigma_{xy}}{\partial x} &= 0, \end{aligned} \tag{5}$$

In this paper, we consider that the elastic modulus and thermal expansion coefficient vary with temperature, thus the constitutive equation can be expressed as

$$\begin{aligned} \varepsilon_x &= \frac{1}{E(T)}(\sigma_x - \mu\sigma_y) + \lambda(T)T, \\ \varepsilon_y &= \frac{1}{E(T)}(\sigma_y - \mu\sigma_x) + \lambda(T)T, \\ \gamma_{xy} &= \frac{2(1+\mu)}{E(T)}\sigma_{xy}, \end{aligned} \tag{6}$$

where $\varepsilon, \gamma, \sigma, u(v), \mu, E(T)$ and $\lambda(T)$ denotes linear strain, shear strain, stress component, displacements, poisson's ratio, elastic modulus and thermal expansion coefficient, respectively.

According to the stress function method, if the three stress components are given by the same stress function Θ, then the equilibrium differential equations are automatically satisfied.

$$\sigma_x = \frac{\partial^2 \Theta}{\partial y^2}, \quad \sigma_y = \frac{\partial^2 \Theta}{\partial x^2}, \quad \sigma_{xy} = -\frac{\partial^2 \Theta}{\partial x \partial y}. \tag{7}$$

2.3. General solutions of temperature-dependent properties problems

2.3.1. General solution of temperature field

In order to solve the divergence equation Eq. (2) for temperature field, we point out that there always exist a new function $\Phi(T)$, which satisfies the following equation

$$\Phi(T) = \int \kappa(T)dT, \tag{8}$$

According to chain rule, the first order partial derivative of $\Phi(T)$ to x and y are

$$\begin{cases} \frac{\partial \Phi}{\partial x} = \kappa(T)\frac{\partial T}{\partial x} = -J_{Qx} \\ \frac{\partial \Phi}{\partial y} = \kappa(T)\frac{\partial T}{\partial y} = -J_{Qy} \end{cases}, \tag{9}$$

Substituting Eq. (9) into Eq. (2), and we obtain a classical Laplace equation

$$\frac{\partial^2 \Phi}{\partial x^2} + \frac{\partial^2 \Phi}{\partial y^2} = 0, \tag{10}$$

In the complex plane, the general solution of Eq. (10) can be expressed as follow

$$\Phi = \left[f(z) + \overline{f(z)}\right] = 2Re[f(z)], \tag{11}$$

where $z = x + iy$. Accordingly, by substituting Eq. (11) into Eq. (9), the expression of thermal flux J_Q could be obtained as

$$J_{Qx} - iJ_{Qy} = -2f'(z), \tag{12}$$

2.3.2. General solutions of thermoelastic fields

As we pointed out earlier in Eq. (7), the equilibrium differential equations can be automatically satisfied if the three stress components are given by the same stress function Θ. However, the compatibility equation represented by Θ is extremely complex now, since the elastic modulus and thermal expansion coefficient are both functions of temperature. In order to simplify the compatibility equation, we prove that there exists a new function U (as detailed in Appendix 1) such that the three stress components satisfying the equilibrium differential equation can be re-expressed as

$$\sigma_x = E(T)\frac{\partial^2 U}{\partial y^2}, \sigma_y = E(T)\frac{\partial^2 U}{\partial x^2}, \sigma_{xy} = -E(T)\frac{\partial^2 U}{\partial x \partial y}, \tag{13}$$

Substituting Eq. (13) into Eq. (6), and we have

$$\begin{aligned} \epsilon_x &= \frac{\partial^2 U}{\partial y^2} - \mu\frac{\partial^2 U}{\partial x^2} + \lambda(T)T, \\ \epsilon_y &= \frac{\partial^2 U}{\partial x^2} - \mu\frac{\partial^2 U}{\partial y^2} + \lambda(T)T, \\ \gamma_{xy} &= -2(1+\mu)\frac{\partial^2 U}{\partial x \partial y}, \end{aligned} \tag{14}$$

then substituting Eq. (14) into Eq. (3), the compatibility equation can be finally obtained as

$$\frac{\partial^4 U}{\partial x^4}+2\frac{\partial^4 U}{\partial x^2\partial y^2}+\frac{\partial^4 U}{\partial y^4}=-\frac{\partial^2}{\partial x^2}[\lambda(T)T]-\frac{\partial^2}{\partial y^2}[\lambda(T)T], \tag{15}$$

Eq. (15) is a fourth-order inhomogeneous partial differential equation, and it's analytical solution is

$$U=U_p+U_s, \tag{16}$$

where U_p denotes particular solution and U_s denotes general solution. Observing Eq. (15), and it becomes clear that the left side of this equation is fourth-order, while the right side of this equation is second-order. Therefore, in order to obtain U_p simply, Eq. (15) can be reduced to a second order partial differential equation

$$\frac{\partial^2 U_p}{\partial z\partial\bar{z}}=-\lambda(T)T, \tag{17}$$

Of course, U_s is still the general solution of the original equation, which could be expressed as

$$U_s=\mathrm{Re}[\bar{z}\varphi(z)+\theta(z)], \tag{18}$$

Now the stress components could be rewritten as

$$\begin{aligned}&\sigma_x+\sigma_y=4E(T)\left[\tfrac{\partial^2 U_p}{\partial z\partial\bar{z}}+\mathrm{Re}[\varphi'(z)]\right],\\&\sigma_y-\sigma_x+2i\sigma_{xy}=2E(T)\left[2\tfrac{\partial^2 U_p}{\partial z^2}+\bar{z}\varphi''(z)+\psi'(z)\right],\end{aligned} \tag{19}$$

and displacement components could be obtained by substituting Eqs. (4) and (18) into Eq. (13)

$$u+iv=(u_s+iv_s)+(u_p+iv_p), \tag{20}$$

where

$$\begin{aligned}&u_s+iv_s=(3-\mu)\varphi(z)-(1+\mu)\left[z\overline{\varphi'(z)}+\overline{\psi(z)}\right],\\&u_p+iv_p=3\int\tfrac{\partial^2 U_p}{\partial z\partial\bar{z}}dx+3i\int\tfrac{\partial^2 U_p}{\partial z\partial\bar{z}}dy-2(1+\mu)\tfrac{\partial U_p}{\partial\bar{z}},\end{aligned} \tag{21}$$

As such, if the particular solution U_p and general solution U_s can be derived, the fields of stress and displacement can then be determined, and the problem is completely solved.

2.4. Boundary condition

The thermal boundary condition at the insulation surface of this elliptical cavity is

$$\int_P^Q J_{Qr}ds=0, \tag{22}$$

where P and Q are arbitrary points given on the boundary and r in Eq. (22) means perpendicular to the boundary surface. Substituting Eq. (9) and Eq. (11) into Eq. (22), we obtain

$$\int_P^Q J_{Qr}ds=\int_P^Q J_{Qy}dx-J_{Qx}dy=\int_P^Q if'(z)dz-i\overline{f'(z)}d\bar{z}=0, \tag{23}$$

Thus

$$\mathrm{Re}[if(z)]=Cons, \tag{24}$$

along the boundary surface.

The elliptical cavity surface is stress free, thus

$$\begin{aligned}&l(\sigma_x)_s+m(\tau_{xy})_s=0,\\&m(\sigma_y)_s+l(\tau_{xy})_s=0,\end{aligned} \tag{25}$$

where l and m are

$$l=\frac{dy}{ds},\quad m=-\frac{dx}{ds}, \tag{26}$$

s here represents a segment of an arc along the boundary. Substituting Eqs. (13) and (26) into Eq. (25) yields

$$\frac{dy}{ds}\left(\frac{\partial^2 U}{\partial y^2}\right)_s+\frac{dx}{ds}\left(\frac{\partial^2 U}{\partial x\partial y}\right)=0, \tag{27}$$

Then substituting Eq. (16) and Eq. (17) into Eq. (24), the stress boundary condition can be finally expressed as

$$\overline{\varphi(z)}+\bar{z}\varphi'(z)+\psi(z)=-2\frac{\partial U_p}{\partial z}. \tag{28}$$

along the boundary surface.

3. Solutions for temperature and thermal flux fields

To be specific, we consider an elliptical cavity embedded in an infinite medium, as shown in Fig. 1a, where a and b denote the lengths of the major and minor semi-axes of the ellipse, and the origin of the coordinate system is located at the center of the elliptical cavity. At the far field, the medium is subjected to imposed thermal flux J_{Qx}^{∞} and J_{Qy}^{∞}.

We adopt the following transforms for the subsequent analysis

$$z(w)=R\left(w+\frac{m}{w}\right), \tag{29}$$

where $R=\frac{a+b}{2}, m=\frac{a-b}{a+b}, w=\frac{z+\sqrt{z^2-4mR^2}}{2R}$, which maps the elliptical cavity in z-plane into an unit circle in w-plane(as shown in Fig. 1b).

Before solving the problem, we first point out that the remote thermal flux is actually determined by the remote thermal conductivity and temperature gradient. For a medium whose material parameters are temperature-dependent, the remote thermal conductivity and temperature gradient both change with the coordinates, since the remote temperature changes with the coordinates. For detailed description, we denote the remote temperature gradient as

$$\left.\frac{\partial T}{\partial x}\right|_{\infty}=t_x,\left.\frac{\partial T}{\partial y}\right|_{\infty}=t_y, \tag{30}$$

In the far field, substituting Eqs. (11) and (30) into Eq. (9), we obtain

$$\begin{aligned}&\tfrac{\partial\Phi}{\partial x}=f'(z)+\overline{f'(z)}=\kappa_\infty t_x=J_{Qx}^{\infty},\\&\tfrac{\partial\Phi}{\partial y}=if'(z)-i\overline{f'(z)}=\kappa_\infty t_y=J_{Qy}^{\infty},\end{aligned} \tag{31}$$

where κ_∞ denotes the remote thermal conductivity. Again we point out that the remote thermal conductivity and temperature gradient both change with the coordinates, while the product of the two, the remote thermal flux is constant. Eq. (31) could be combined as

$$\frac{\kappa_\infty}{2}(t_x-it_y)=f'(\infty), \tag{32}$$

thus we have

$$f(z)=\frac{\kappa_\infty}{2}(t_x-it_y)z+f_0(z), \tag{33}$$

where $f_0(z)$ satisfies

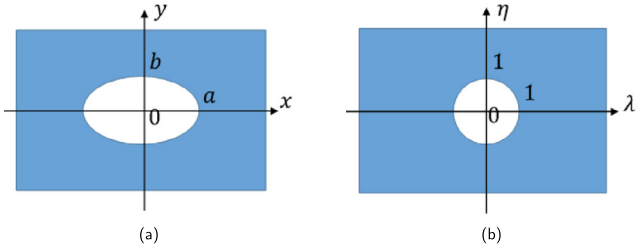

Fig. 1. (a) An elliptical cavity embedded in an infinite matrix, (b) The w-plane after conformal mapping.

$$\lim_{z\to\infty} f_0(z) = 0, \tag{34}$$

In order to cipher out the concrete form of $f_0(z)$, we rewrite $f(z)$ by substituting Eq. (29) into Eq. (33) as

$$f(z) = \frac{R\kappa_\infty}{2}(t_x - it_y)w + \frac{mR\kappa_\infty}{2}(t_x - it_y)\frac{1}{w} + f_0(z), \tag{35}$$

Then substituting Eq. (35) into the boundary condition Eq. (24) yields

$$f(z) = Aw + \frac{\overline{A}}{w}, \tag{36}$$

where

$$A = \frac{\kappa_\infty R}{2}(t_x - it_y), \tag{37}$$

Substituting Eq. (36) into Eq. (12), the thermal flux could be finally obtained as

$$J_{Qx} - iJ_{Qy} = \frac{2\left(\overline{A} - Aw^2\right)}{R(w^2 - m)}, \tag{38}$$

Here we can see that the expression of heat flux is very concise, and is consistent with the temperature independent case. In other words, the temperature dependence of thermal conductivity does not affect the thermal flux distribution when the remote thermal flux is certain. Substituting Eq. (36) into Eq. (11), the equation that determine the temperature field is

$$\int \kappa(T)dT = 2\mathrm{Re}\left[Aw + \frac{\overline{A}}{w}\right], \tag{39}$$

The right side of the above equation is the known function which has been obtained, and the left side is the function of temperature. Obviously, the final expression of temperature field depends on the concrete form of $\kappa(T)$. In most cases, the form of $\kappa(T)$ needs to be fitted from the experimental data. For simplicity, we expand $\kappa(T)$ to a polynomial of temperature, thus

$$\kappa(T) = \sum_i^n \kappa_i T^i, \tag{40}$$

where κ_i are known coefficients determined by experimental data. In this case, Eq. (39) will be transformed into a polynomial equation, and the final temperature field can be obtained by using the polynomial root formula. For example, when other coefficients are zero except κ_0 and κ_2, the temperature field could be finally expressed as

$$T = \frac{\mathrm{Re}[f(z)]}{\kappa_0} - \frac{\sqrt{[(1 + w\bar{w})\mathrm{Re}[Aw]]^2 - \bar{w}^2 w^2 \kappa_0 \kappa_2}}{w\bar{w}\kappa_0}. \tag{41}$$

4. Solutions for stress fields

4.1. Particular solution and general solution

Observing Eq. (17), it is clear that the term $-\lambda(T)T$ is a known function with respect to temperature, and can be expanded to a polynomial of temperature according to the experimental data. However, due to the complexity of the expression of temperature field itself, it is not a good choice to expand the right side of Eq. (17) as the series of temperature. Noting that $\Phi(T)$ is also a known function with respect to temperature (see Eq. 8), and its expression is much more concise, so we choose to expand the right side of Eq. (17) as the series of $\Phi(T)$

$$\lambda(T) = \sum C_k \Phi^k(T), \tag{42}$$

To be specific, we choose the following non-linear relationship for the later calculation

$$-\lambda(T)T = c_0 + c_1\Phi(T) + c_2\Phi^2(T), \tag{43}$$

where c_0, c_1 and c_2 are known fitting coefficients according to the experimental data. Combining Eqs. (11), (17) and (43), we obtain

$$\frac{\partial U_p}{\partial z \partial \bar{z}} = c_0 + 2c_1\mathrm{Re}[f(z)] + 4c_2\mathrm{Re}[f(z)]^2, \tag{44}$$

and

$$U_p = c_0 z\bar{z} + c_1\left[\bar{z}F(z) + z\overline{F(z)}\right] + c_2\left[\bar{z}\int f^2(z)dz + 2F(z)\overline{F(z)} + z\int \overline{f^2(z)}d\bar{z}\right], \tag{45}$$

where $F(z)$ denotes the primitive function of $f(z)$

$$F(z) = \frac{AR}{2}w^2 + \frac{\bar{A}Rm}{2}\frac{1}{w^2} + R(\bar{A} - Am)\ln w, \tag{46}$$

Substituting Eqs. (36) and (46) into Eq. (45), and then take the first derivative of U_p, thus leads to the expression of $\frac{\partial U_p}{\partial z}$ along the elliptic surface

$$\left.\frac{\partial U_p}{\partial z}\right|_\zeta = \sum_{k=-3}^{3}\alpha_k\zeta^k + \ln\sigma\sum_{k=-1}^{1}\beta_k\zeta^k + c_2\int\overline{f^2(z)}d\bar{z}, \tag{47}$$

where

$$\begin{cases}\alpha_{-3} = -4R\bar{A}^2c_2\\ \alpha_{-2} = -3c_1R\bar{A}\\ \alpha_{-1} = -3R\left[c_2R\bar{A}(m\bar{A} + 3A) + c_0\right]\end{cases}, \quad \begin{cases}\alpha_0 = -3R(A + m\bar{A})c_1\\ \alpha_1 = -3R\left[mc_0 + A(A + 3m\bar{A})c_2\right]\\ \alpha_2 = -3AmRc_1\\ \alpha_3 = -4A^2mRc_2\end{cases}, \tag{48}$$

and

$$\begin{cases}\beta_{-1} = 4\bar{A}Rc_2(A - m\bar{A})\\ \beta_0 = 2Rc_1(A - m\bar{A})\\ \beta_1 = 4ARc_2(A - m\bar{A})\end{cases}, \tag{49}$$

where ζ denotes w along the elliptic surface.

Substituting Eq. (47) and Eq. (29) into Eq. (28), and the stress boundary condition could be finally expressed as

$$\overline{\varphi(\zeta)} + \frac{\overline{z(\zeta)}}{z'(\zeta)}\varphi'(\zeta) + \psi(\zeta) = -2\left[\sum_{k=-3}^{3}\alpha_k\zeta^k + \ln\sigma\sum_{k=-1}^{1}\beta_k\zeta^k + c_2\int\overline{f^2(z)}d\bar{z}\right], \tag{50}$$

where

$$\frac{\overline{z(\zeta)}}{z'(\zeta)} = \frac{\bar{\zeta}^2 + m}{\bar{\zeta} - m\bar{\zeta}^3} = \frac{\zeta + m\zeta^3}{\zeta^2 - m}, \tag{51}$$

According to the stress boundary condition and the remote condition, $\varphi(w)$ could be selected as

$$\varphi(w) = \sum_{k=-3}^{3}\frac{\bar{\alpha}_k}{w^k} + c_2\int f^2(z)dz, \tag{52}$$

Then the expression of $\psi(w)$ could be obtained by substituting Eqs. (51), (47) and (52) into Eq. (28) as

$$\psi(w) = \ln w\sum_{k=-1}^{1}\beta_k w^k - \frac{w + mw^3}{w^2 - m}\left(\sum_{k=-3}^{3}\frac{-k\bar{\alpha}_k}{w^{k+1}} + c_2z'(w)f^2(z)\right). \tag{53}$$

$\varphi(w)$ and $\psi(w)$ are general solutions of the compatible equation added to satisfy the stress boundary condition. However, they are not the general solutions of the final form, since the single value conditions have not been considered.

4.2. Stress and displacement single value conditions

In order to satisfy the single-valued condition of stress, it is necessary to list the multivalued parts of stress components. Observing Eq. (19), and it could be obtained from Eqs. (45), (51) and (52) that $\frac{\partial^2 U_p}{\partial z \partial \bar{z}}$ and $\varphi''(z)$ are both single-valued, while $\frac{\partial^2 U_p}{\partial z^2}$ and $\psi'(z)$ are multi-valued

$$\begin{aligned} &\frac{\partial^2 U_p}{\partial z^2} = d_1 \ln \bar{w} + d_2 \frac{\ln w}{w^2}, \\ &\psi_1'(z) = d_3 \ln w + d_4 \frac{\ln w}{w^2}, \end{aligned} \tag{54}$$

where

$$\begin{cases} d_1 = \frac{\beta_1}{2z'(w)} \\ d_2 = -\frac{\beta_{-1}}{2z'(w)} \end{cases}, \quad \begin{cases} d_3 = \frac{\beta_1}{z'(w)} \\ d_4 = -\frac{\beta_{-1}}{z'(w)} \end{cases}, \tag{55}$$

Substituting Eq. (54) into Eq. (19), and we could obtain the multivalued part of stress components.

$$\left(\sigma_y - \sigma_x + 2i\sigma_{xy}\right)\big|_{mult} = 2E(T)\left[(d_3 - 2d_1)i\theta + (d_4 - 2d_2)\frac{i\theta}{w^2}\right], \tag{56}$$

according to Eq. (55) we have $d_3 = 2d_1$ and $d_4 = 2d_2$, thus it can be concluded that the single stress condition is satisfied automatically.

The displacement components can be expressed through substituting Eqs. (52), (53) and (45) into Eq. (21). Here we only need to give their multivalued terms

$$\begin{aligned} u &= 2\mathrm{Re}[g_1 \ln w] + y \cdot 2\mathrm{Re}[g_2 \ln w], \\ v &= 2\mathrm{Re}[-ig_1 \ln w] + x \cdot 2\mathrm{Re}[g_2 \ln w], \end{aligned} \tag{57}$$

or

$$u + iv = 2(g_1 - \bar{g}_1)i\theta + \bar{z}(ig_2 - i\bar{g}_2)i\theta, \tag{58}$$

where

$$\begin{aligned} g_1 &= -4c_1 R(mA - \bar{A}), \\ g_2 &= i8c_2\left(\bar{A} + \tfrac{A}{m}\right)\left(A - \tfrac{\bar{A}}{m}\right), \end{aligned} \tag{59}$$

A new general solution $\varphi_2(w)$ and $\psi_2(w)$ is introduced to ensure that the final displacement is singular. Obviously, it still needs to satisfy the stress boundary condition, which require

$$\varphi_2(\zeta) + \frac{z(\zeta)}{\overline{z'(\zeta)}}\overline{\varphi_2'(\zeta)} + \overline{\psi_2(\zeta)} = 0, \tag{60}$$

According to Eq. (58), the expression of additional general solution $\varphi_2(w)$ could be selected as

$$\varphi_2(w) = k_1 \ln w + k_2 z \ln w, \tag{61}$$

Substituting Eq. (61) into Eq. (60), and we could obtain the expression of $\psi_2(w)$

$$\begin{aligned} \psi_2(w) = &\left(\bar{k}_2 - k_2\right)R\left(mw + \frac{1}{w}\right)\ln w - k_2 R \\ &\times \frac{(w^2 + m)(1 + mw^2)}{w(w^2 - m)}, \end{aligned} \tag{62}$$

In order to ensure that the additional general solution $\varphi_2(w)$ and $\psi_2(w)$ satisfy the single stress condition, the coefficient k_2 must satisfy

$$k_2 - \bar{k}_2 = 0, \tag{63}$$

Finally, in order to cancel out the multivalued displacement, we combine Eqs. (61), (62), (63) and (58), noting that $y \cdot \ln w$ is single-valued (as proven in our previous paper (Song et al., 2020)), then k_1 and k_2 could be obtained as

$$\begin{aligned} k_1 &= \tfrac{2(g_1 - \bar{g}_1)}{1 - 3\mu}, \\ k_2 &= \tfrac{ig_2 - i\bar{g}_2}{4}, \end{aligned} \tag{64}$$

and the two stress functions could be finally concluded as

$$\begin{aligned} \varphi(w) &= \sum_{k=-3}^{3} \frac{\bar{\alpha}_k}{w^k} + c_2 \int f^2(z)dz + (k_1 + k_2 z)\ln w, \\ \psi(w) &= \ln w \sum_{k=-1}^{1} \beta_k w^k - \tfrac{w + mw^3}{w^2 - m}\left[\sum_{k=-4}^{2} \chi_k w^k\right], \end{aligned} \tag{65}$$

where

$$\begin{cases} \chi_{-4} = -mR\bar{A}^2 c_2 - 3\bar{\alpha}_3 \\ \chi_{-3} = -2\bar{\alpha}_2 \\ \chi_{-2} = -\bar{\alpha}_1 - 2Ac_2 mR\bar{A} + c_2 R\bar{A}^2 + k_2 Rm \end{cases}, \quad \begin{cases} \chi_{-1} = 0 \\ \chi_0 = -A^2 mRc_2 + 2AR\bar{A}c_2 + \bar{\alpha}_{-1} + k_2 R \\ \chi_1 = 2\bar{\alpha}_{-2} \\ \chi_2 = A^2 Rc_2 + 3\bar{\alpha}_{-3} \end{cases}. \tag{66}$$

This set of equations solves the problems completely, leading to the full determination of the field distributions around the elliptic cavity. Here we emphasize that both the particular solution U_p and General solution U_s (i.e. $\varphi(w)$ and $\psi(w)$) are linear functions of c_0, c_1 and c_2 , so the final stress components are all linear functions of c_0, c_1 and c_2 .

5. Solutions for crack

For the special case of a crack with $b/a \to 0, m \to 1$ and $R \to a/2$, the stress intensity factors of the right crack tip are worth studied, and the expression of stress intensity factors K could be written as

$$K_1 - iK_2 = 2\sqrt{2\pi}E_t \lim_{z \to a} \sqrt{z - a}\varphi'(z), \tag{67}$$

where E_t denotes the elastic modulus at the right crack tip, and $\varphi'(z)$ could be deduced from Eq. (65) as:

$$\begin{aligned} \varphi'(z) &= \frac{\varphi'(w)}{z'(w)} \\ &= \frac{2w^2}{a(w^2 - 1)}\left[\sum_{k=-4}^{2} \delta_k w^k + \frac{ak_2}{2}\left(1 - \frac{1}{w^2}\right)\ln w\right] + c_2 f^2(z), \end{aligned} \tag{68}$$

where

$$\begin{cases} \delta_{-4} = -3\bar{\alpha}_3 \\ \delta_{-3} = -2\bar{\alpha}_2 \\ \delta_{-2} = \frac{ak_2}{2} - \bar{\alpha}_1 \end{cases}, \quad \begin{cases} \delta_{-1} = k_1 \\ \delta_0 = \frac{ak_2}{2} + \bar{\alpha}_{-1} \\ \delta_1 = 2\bar{\alpha}_{-2} \\ \delta_2 = 3\bar{\alpha}_{-3} \end{cases}, \tag{69}$$

Substituting Eq. (68) into Eq. (67), thus

$$K_s = K_1 - iK_2 = 2\sqrt{\frac{\pi}{a}}E_t \sum_{k=-4}^{2} \delta_k, \tag{70}$$

Eq. (70) could also be divided into 3 parts:

$$K_s = K_{1s} + K_{2s} + K_{3s}, \tag{71}$$

where

$$
\begin{aligned}
K_{1s} &= 3ic_1\sqrt{\pi}a^{3/2}\kappa_\infty E_t t_y,\\
K_{2s} &= \tfrac{3}{8}c_2\sqrt{\pi}a^{5/2}\kappa_\infty^2 E_t\left(2t_x^2+t_y^2+9it_xt_y\right),\\
K_{3s} &= -\tfrac{3}{16}c_2\sqrt{\pi}a^{7/2}\kappa_\infty^2 E_t\left(2t_x^2+t_y^2-it_xt_y\right).
\end{aligned}
\tag{72}
$$

It can be seen from Eq. (70) to Eq. (72) that K_1 and K_2 are significantly different from the classical temperature independent case. Firstly, the stress intensity factors have nonlinear terms with respect to the remote thermal loads. Secondly, the stress intensity factors now depends on $a^{3/2}, a^{5/2}$ and $a^{7/2}$. Thirdly, type 1 intensity factor K_1 may exist, although its value is much smaller then that of K_2.

6. Numerical results and discussions

In this section, we use numerical examples to verify the analytical results and search for valuable and meaningful results. Assuming that the medium is Steel Alloy, with the corresponding material parameters are showed in Table 1, and the size of this elliptic cavity are $a = 0.01$ m, $b = 0.004$ m.

6.1. Contours of temperature and stress components

We first plot the contours of temperature in Fig. 2. It can be seen that once the thermal conductivity changes with temperature, the temperature distribution will be visible different from the classical results. Although there is only about 50 degree temperature difference in the calculation area, and the corresponding thermal conductivity change is only 5 percents. Through the comparison of the three figures, it can be seen that the temperature distribution in the calculation range becomes more complex and the temperature difference becomes larger after the material properties are considered as temperature dependence.

We then calculate the contours of thermal stress in Figs. 3–5, where the thermal expansion coefficient are set to be constant (a), linear function of temperature (b) and nonlinearly function of temperature (c). It is seen that when the material properties are temperature dependent, the distribution of σ_x and σ_y has a visible change compared with the classical results, while the distribution of σ_{xy} does not change much. In addition, when the thermal expansion coefficient is a nonlinear function of temperature, all the absolute values of the three stress components at the right end of the

Table 1
Material parameters of 45 carbon steel.

Temperature (K)	293.15	373.15	473.15	573.15	673.15	773.15	873.15	973.15
κ (T) (W/mK)			46.9	45.2	42.3	39.4	35.5	31
$\lambda(T)10^{-6}$ (1/K)		11.7	12.43	13.13	13.67	14.10	14.47	14.76
$E(T)10^5$ (MPa)	2.09	2.07	2.02	1.96	1.85	1.74	1.63	

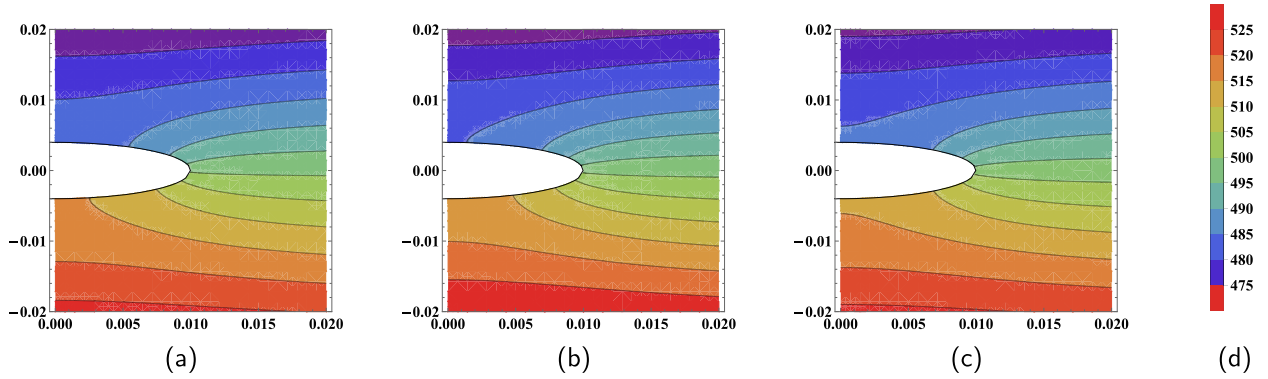

Fig. 2. Distribution of temperature fields around the cavity under the assumption of thermal conductivity being (a) constant, (b) linearly with temperature, (c) nonlinearly with temperature, (d) Plotlegend.

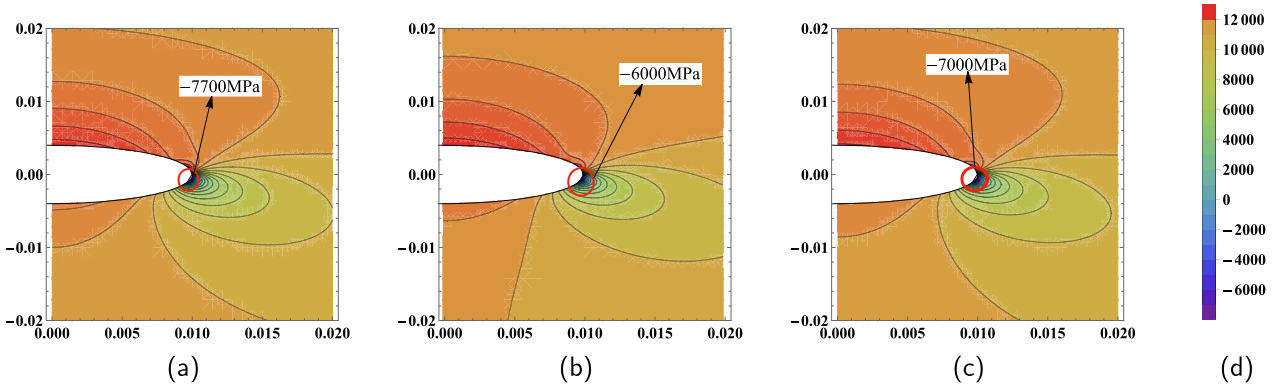

Fig. 3. Distribution of σ_x around the cavity under the assumption of: (a) material parameters being constant, (b) thermal expansion linearly with temperature, (c) thermal expansion nonlinearly with temperature, (d) Plotlegend of σ_x.

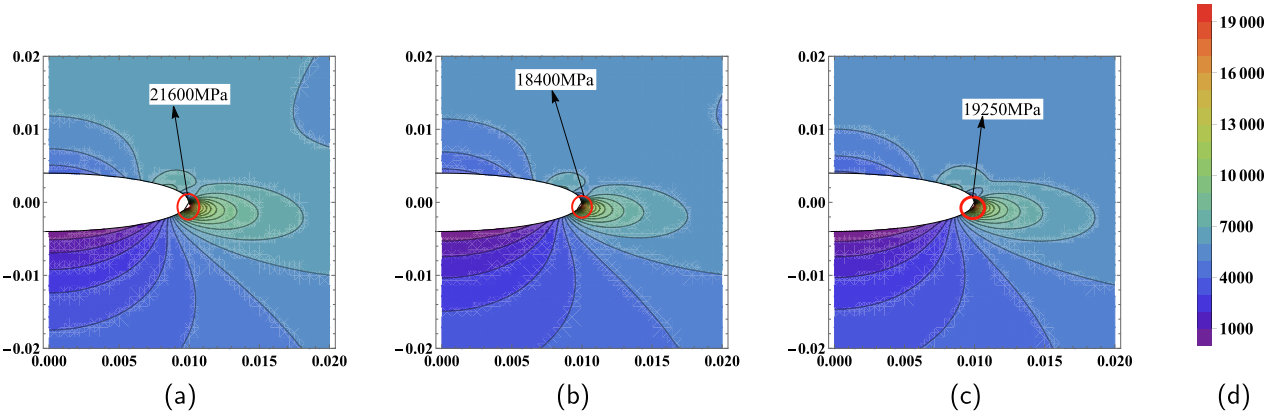

Fig. 4. Distribution of σ_y around the cavity under the assumption of (a) material parameters being constant, (b) thermal expansion linearly with temperature, (c) thermal expansion nonlinearly with temperature, (d) Plotlegend of σ_y.

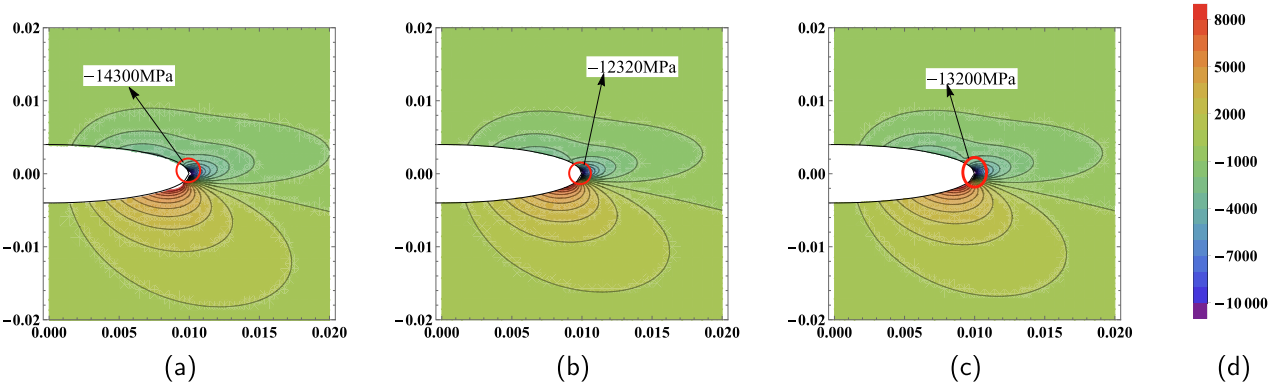

Fig. 5. Distribution of σ_{xy} around the cavity under the assumption of (a) material parameters being constant, (b) thermal expansion linearly with temperature, (c) thermal expansion nonlinearly with temperature, (d) Plotlegend of σ_{xy}.

elliptical cavity are about 10 percent smaller than those of the classical cases.

6.2. Stress concentration at right tip

To further appreciate the relationship between the maximum stress and form of thermal expansion coefficient, we also show in Fig. 6 the maximum mises stress σ_s varies the geometric parameter a/b,with the semiminor axis b fixed as 0.004. It can be seen from Fig. 6 that σ_s changes nonlinearly with a/b. when a/b is less than 1, the stress changes slowly with the increase of a/b. But then, σ_s increases more and more quickly, especially when $a/b > 2$, mainly because the curvature of the right end increases rapidly. In addition, compared with the classical results, the value of σ_s becomes slightly smaller when the material properties are considered as temperature dependence.

Finally, we show the variation of the thermal stress intensity factors with crack length and remote thermal load in Figs. 7 and 8. It can be seen that when the material properties are temperature dependent, K_1 has a small negative value, which is significantly different from the classical result that K_1 is always zero, and indicates that thermal flux can actually close the crack slightly. In addition, both K_1 and K_2 vary nonlinearly with remote thermal load.

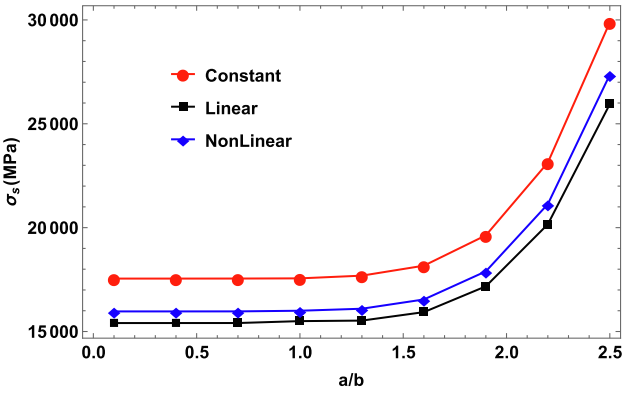

Fig. 6. The mises stress at the cavity tip versus geometric parameter under the assumption of (a) material parameters being constant, (b) thermal expansion linearly with temperature and (c) thermal expansion nonlinearly with temperature.

7. Concluding rremarks

The thermal-elastic problem of an elliptic cavity embedded in an infinite medium has been analyzed in this paper, with the temperature dependence of thermal conductivity, elastic modulus and thermal expansion coefficient fully accounted for. The temperature, thermal flux and thermal stress distributions have been obtained, and the following results can be summarized:

1. The analytical results indicate that the thermal flux distribution is consistent with the temperature independent case. In other words, the temperature dependence of thermal conductivity

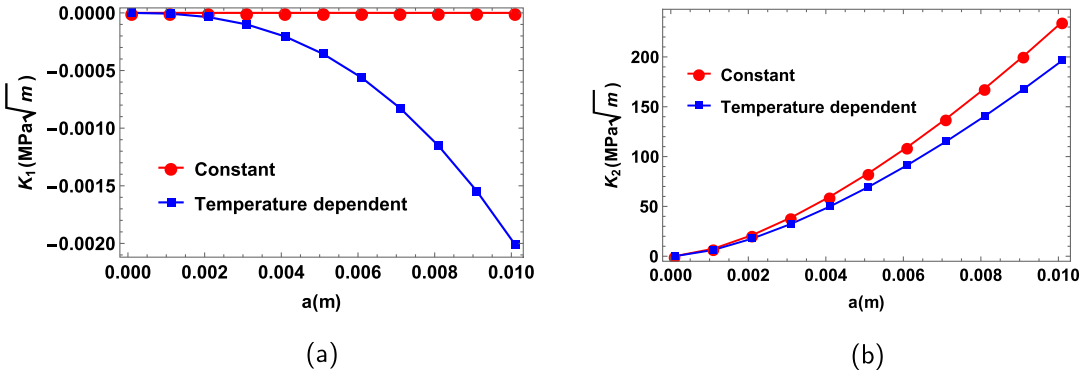

Fig. 7. Stress intensity factors K_1 (a) and K_2 (b) versus half crack length under the assumption of material parameters being constant and temperature dependent respectively.

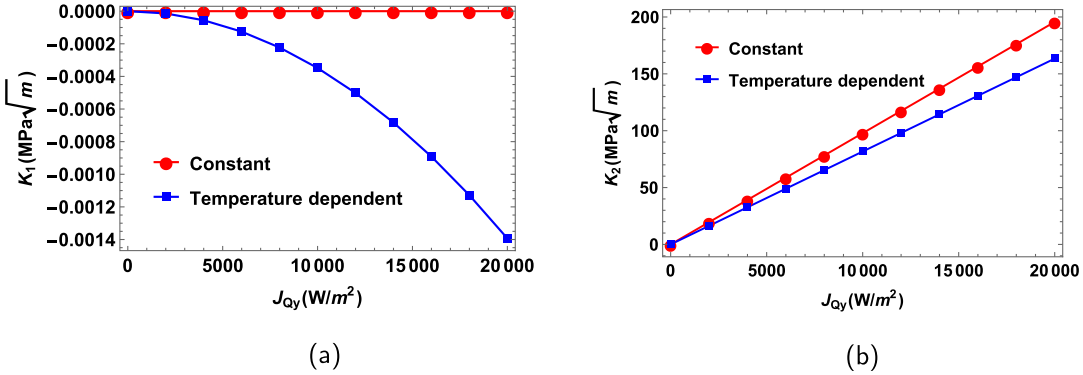

Fig. 8. Stress intensity factors K_1 (a) and K_2 (b) versus remote thermal flux (J_{Qy}) under the assumption of material parameters being constant and temperature dependent respectively.

does not affect the thermal flux distribution when the remote thermal flux is certain.

2. K_1 and K_2 are significantly different from the classical temperature independent case. Firstly, the stress intensity factors have nonlinear terms with respect to the remote thermal loads. Secondly, the stress intensity factors now depends on $a^{3/2}, a^{5/2}$ and $a^{7/2}$. Thirdly, type 1 intensity factor K_1 may exist, although its value is much small then that of K_2.
3. The analysis shows that thermal flux solution is consistent with the temperature independent case, while the temperature and thermal stress solutions are much more complicated.
4. All the three stress components vary linearly with c_0, c_1 and c_2. The maximum mises stress σ_s varies nonlinearly with c_0 and c_1, which is caused by the nonlinear relationship between σ_s and stress components.
5. K_1 has a tiny negative value, which indicates that thermal flux can actually close the crack slightly. In addition, both K_1 and K_2 vary nonlinearly with remote thermal loads.
6. Both K_1 and K_2 increase with the increase of crack length, and the increase of K_2 is less obvious when the temperature dependence of material properties is considered.

Declaration of Competing Interest

The authors declare that they have no known competing financial interests or personal relationships that could have appeared to influence the work reported in this paper.

Acknowledgment

The work was supported by the Fundamental Research Funds for the Central Universities NS2019004.

Appendix A

In order to simplify the compatible equation, we point out that there always exists two functions U_1 and g_1, which satisfy

$$\frac{\partial^2 U_1}{\partial x \partial y} = g_1'\left(\frac{\partial \Theta}{\partial x}\right)\frac{\partial^2 \Theta}{\partial x \partial y} = \frac{1}{E(T)}\frac{\partial^2 \Theta}{\partial x \partial y}, \tag{A.1}$$

Thus it could be obtained from Eq. (A.1) that:

$$\frac{\partial U_1}{\partial x} = g_1\left(\frac{\partial \Theta}{\partial x}\right), \tag{A.2}$$

and

$$\frac{\partial^2 U_1}{\partial x^2} = g_1'\left(\frac{\partial \Theta}{\partial x}\right)\frac{\partial^2 \Theta}{\partial x^2} = \frac{1}{E(T)}\frac{\partial^2 \Theta}{\partial x^2}, \tag{A.3}$$

Similarly, there always exists two functions U_2 and g_2, which satisfy

$$\frac{\partial^2 U_2}{\partial x \partial y} = g_2'\left(\frac{\partial \Theta}{\partial x}\right)\frac{\partial^2 \Theta}{\partial x \partial y} = \frac{1}{E(T)}\frac{\partial^2 \Theta}{\partial x \partial y}, \tag{A.4}$$

and

$$\frac{\partial^2 U_2}{\partial y^2} = g_2'\left(\frac{\partial \Theta}{\partial y}\right)\frac{\partial^2 \Theta}{\partial y^2} = \frac{1}{E(T)}\frac{\partial^2 \Theta}{\partial y^2}, \tag{A.5}$$

It could be learned from above Eqs. (72) and (A.3) that:

$$\frac{\partial^2 U_2}{\partial x \partial y} = \frac{\partial^2 U_1}{\partial x \partial y}, \tag{A.6}$$

Integrating Eq. (A.8), and we have:

$$U_1 = U_2 + f_1(x) + f_2(y) + Cons, \tag{A.7}$$

Obviously, U_1 and U_2 can only differ from functions of single variable with respect to x or y. Therefore, in most complex problems, that is, when the solutions of U_1 and U_2 do not contain the univariate functions of x or y, we have

$$U = U_1 = U_2, \tag{A.8}$$

In these cases, substituting Eq. (72), Eq. (A.2), Eqs. (A.4), (A.5) and (A.7) into Eq. (7) and we have

$$\sigma_x = E(T)\frac{\partial^2 U}{\partial y^2}, \sigma_y = E(T)\frac{\partial^2 U}{\partial x^2}, \sigma_{xy} = -E(T)\frac{\partial^2 U}{\partial x \partial y}. \tag{A.9}$$

Here we emphasize that in fact U_1 and U_2 can contain linear functions of x and y, which will not affect the establishment of Eq. (A.8), since the expressions of stress components takes the second partial derivative of U.

References

Abbas, I., 2014. Nonlinear transient thermal stress analysis of thick-walled fgm cylinder with temperature-dependent material properties. MECCANICA 49, 1697–1708.

Abbas, I., Youssef, H., 2012. A nonlinear generalized thermoelasticity model of temperature-dependent materials using finite element method. Int. J. Thermophys. 33, 1302–1313.

Abbas, I.A., 2014. Eigenvalue approach in a three-dimensional generalized thermoelastic interactions with temperature-dependent material properties. Comput. Math. Appl. 68, 2036–2056.

Abbas, I.A., Marin, M., 2017. Analytical solution of thermoelastic interaction in a half-space by pulsed laser heating. Physica E 87, 254–260.

Aksamija, Z., Knezevic, I., 2011. Lattice thermal conductivity of graphene nanoribbons: anisotropy and edge roughness scattering. Appl. Phys. Lett. 98, 141919.

Alonso, D., Artuso, R., Casati, G., Guarneri, I., 1999. Heat conductivity and dynamical instability. Phys. Rev. Lett. 82, 1859–1862.

Dag, S., 2007. Mixed-mode fracture analysis of functionally graded materials under thermal stresses: a new approach using j(k)-integral. J. Therm. Stresses 30, 269–296.

Dag, S., Erhan Arman, E., Yildirim, B., 2010. Computation of thermal fracture parameters for orthotropic functionally graded materials using jk-integral. Int. J. Solids Struct. 47, 3480–3488.

Dag, S., Yildirim, B., Topal, S., 2013. Computational methods for inclined cracks in orthotropic functionally graded materials under thermal stresses. J. Therm. Stresses 36, 1001–1026.

Ezzat, M., El-Karamany, A., Samaan, A., 2004. The dependence of the modulus of elasticity on reference temperature in generalized thermo elasticity with thermal relaxation. Appl. Math. Comput. 147, 169–189.

Ezzat, M.A., Awad, E.S., 2010. Constitutive relations, uniqueness of solution, and thermal shock application in the linear theory of micropolar generalized thermoelasticity involving two temperatures. J. Therm. Stresses 33, 226–250.

Ezzat, M.A., El-Karamany, A.S., El-Bary, A.A., 2014. Generalized thermo-viscoelasticity with memory-dependent derivatives. Int. J. Mech. Sci. 89, 470–475.

Florence, A.L., Goodier, J.N., 1960. Thermal stresses due to disturbance of uniform heat flow by an insulated ovaloid hole. J. Appl. Mech. 27, 635–639.

Hasebe, N., Wang, X., 2005. Complex variable method for thermal stress problem. J. Therm. Stresses 28, 595–648.

Huaijie, C., Ding-Bang, X., Zhanqiu, T., Genlian, F., Zhiqiang, L., Qiang, G., Yishi, S., Cuiping, G., Di, Z., 2018. Thermal properties of in situ grown graphene reinforced copper matrix laminated composites. J. Alloys Compds. S0925838818331669–..

Li, N., Ren, J., Wang, L., Zhang, G., Hnggi, P., Li, B., 2012. Colloquium: phononics: manipulating heat flow with electronic analogs and beyond. Rev. Mod. Phys. 84, 1045–1066.

Liu, P.S., 2003. Status of study on high-temperature oxidation law for aluminide coatings. Rare Met. Mater. Eng. 32, 681–685.

Liu, S., Xu, X.F., Xie, R.G., Zhang, G., Li, B.W., 2012. Anomalous heat conduction and anomalous diffusion in low dimensional nanoscale systems. Eur. Phys. J. B 85.

Molian, R., Shrotriya, P., Molian, P., 2008. Thermal stress fracture mode of co2 laser cutting of aluminum nitride. Int. J. Adv. Manuf. Technol. 39, 725–733.

Rajabi, M., Soltani, N., Eshraghi, I., 2016. Effects of temperature dependent material properties on mixed mode crack tip parameters of functionally graded materials. Struct. Eng. Mech. 58, 217–230.

Sherief, H.H., Ezzat, M.A., 1994. Solution of the generalized problem of thermoelasticity in the form of series of functions. J. Therm. Stresses 17, 75–95.

Sih, G.C., 1965. Heat conduction in the infinite medium with lines of discontinuities. J. Heat Transfer 87, 293.

Sih, G.C., 1962. On the singular character of thermal stresses near a crack tip. J. Appl. Mech. 29, 3724–3731.

Song, H., Xie, K., Gao, C., 2020. Progressive thermal stress distribution around a crack under joule heating in orthotropic materials. Appl. Math. Model. 86, 271–293.

Wilson, W., Yu, I., 1979. The use of the j-integral in thermal stress crack problems. Int. J. Fract. 15, 377–387.

Xie, H., Hu, M., Bao, H., 2014. Thermal conductivity of silicene from first-principles. Appl. Phys. Lett. 104, 131906.

Xie, K., Song, H., Gao, C., 2019. Electric and heat conduction across an elliptic cavity in an anisotropic medium. Math. Mech. Solids 24, 3279–3294.